AGU PUBLICATIONS

Geophysical Research Letters

RESEARCH LETTER
10.1002/2015GL066848

Key Points:
- Three-dimensional model of Titan's interaction with the supersonic solar wind
- Model can quantitatively explain Cassini magnetic field and plasma data
- Evidence of fossilized solar wind magnetic field in Titan's ionosphere

Correspondence to:
M. Feyerabend,
feyerabend@geo.uni-koeln.de

Citation:
Feyerabend, M., S. Simon, F. M. Neubauer, U. Motschmann, C. Bertucci, N. J. T. Edberg, G. B. Hospodarsky, and W. S. Kurth (2016), Hybrid simulation of Titan's interaction with the supersonic solar wind during Cassini's T96 flyby, *Geophys. Res. Lett.*, *43*, 35–42, doi:10.1002/2015GL066848.

Received 3 NOV 2015
Accepted 18 DEC 2015
Accepted article online 22 DEC 2015
Published online 13 JAN 2016

Hybrid simulation of Titan's interaction with the supersonic solar wind during Cassini's T96 flyby

Moritz Feyerabend[1,2], Sven Simon[2], Fritz M. Neubauer[1], Uwe Motschmann[3,4], Cesar Bertucci[5], Niklas J. T. Edberg[6], George B. Hospodarsky[7], and William S. Kurth[7]

[1]Institute of Geophysics and Meteorology, University of Cologne, Cologne, Germany, [2]School of Earth and Atmospheric Sciences, Georgia Institute of Technology, Atlanta, Georgia, USA, [3]Institute for Theoretical Physics, University of Braunschweig, Braunschweig, Germany, [4]Institute for Planetary Research, German Aerospace Center, Berlin, Germany, [5]Institute for Astronomy and Space Physics, CONICET/University of Buenos Aires, Ciudad Universitaria, Buenos Aires, Argentina, [6]Swedish Institute of Space Physics, Uppsala, Sweden, [7]Department of Physics and Astronomy, University of Iowa, Iowa City, Iowa, USA

Abstract By applying a hybrid (kinetic ions and fluid electrons) simulation code, we study the plasma environment of Saturn's largest moon Titan during Cassini's T96 flyby on 1 December 2013. The T96 encounter marks the only observed event of the entire Cassini mission where Titan was located in the supersonic solar wind in front of Saturn's bow shock. Our simulations can quantitatively reproduce the key features of Cassini magnetic field and electron density observations during this encounter. We demonstrate that the large-scale features of Titan's induced magnetosphere during T96 can be described in terms of a steady state interaction with a high-pressure solar wind flow. About 40 min before the encounter, Cassini observed a rotation of the incident solar wind magnetic field by almost 90°. We provide strong evidence that this rotation left a bundle of fossilized magnetic field lines in Titan's ionosphere that was subsequently detected by the spacecraft.

1. Introduction

The dense atmosphere and ionosphere of Saturn's largest moon Titan (radius $R_T = 2575$ km) lead to a strong interaction with the impinging plasma, which has been sampled during the Voyager 1 flyby and during more than 100 flybys of the Cassini spacecraft. For average solar wind conditions, Titan is located within the outer regions of Saturn's magnetosphere [*Bertucci et al.*, 2009], exposed to the subsonic Kronian magnetospheric plasma. In times of enhanced solar wind dynamic pressure Titan may be located in the magnetosheath or even upstream of Saturn's bow shock and can then interact with solar wind plasma. However, out of the 113 Cassini flybys so far, only two took place while Titan was located in Saturn's magnetosheath. The first of them was the T32 encounter on 13 June 2007. Magnetic field observations from this flyby provided initial confirmation of the existence of fossilized magnetic fields in the convection-dominated region of Titan's ionosphere [*Bertucci et al.*, 2008]. Fossilized field lines are "trapped" in the ionosphere between altitudes of 1800 and 1000 km due to the low plasma velocity of 0.1–1 km/s in this region, compared to ~100 km/s upstream of Titan [*Neubauer et al.*, 2006]. The second Titan flyby in Saturn's magnetosheath was T85 on 24 July 2012. During T85 the Cassini Langmuir Probe (LP) detected the highest electron densities ever measured in Titan's ionosphere, possibly caused by the increased impact ionization due to the energetic magnetosheath particles [*Edberg et al.*, 2013].

The T96 encounter on 1 December 2013 (closest approach altitude of 1400 km at 00:41, 12.4 local time) constitutes the first and only event of the entire Cassini mission where Titan was found in the supersonic solar wind upstream of Saturn's bow shock [*Bertucci et al.*, 2015]. Plasma and magnetic field observations showed that Titan was exposed to unshocked high-pressure solar wind plasma for about 6 h prior to the encounter. About 2 h before closest approach Cassini crossed a sector boundary in the solar wind, followed by significant fluctuations in the direction and magnitude of the solar wind magnetic field. From around 00:00 on, these perturbations weakened significantly after the crossing of a shock front (SF), with the solar wind magnetic field changing from a predominantly west-east orientation to a predominantly north-south orientation. Although this event is apparently not related to Titan, its nature is not yet understood [*Bertucci et al.*, 2015].

The plasma and magnetic data obtained from Titan's interaction region revealed similar features to those known from the induced magnetospheres of Mars and Venus, including the formation of a bow shock and a magnetic barrier at Titan's ramside [see *Bertucci et al.*, 2011]. However, the pileup of the magnetic field at closest approach was found to be too large (~25 nT compared to upstream values of ~1 nT) to be consistent with the dynamic pressure of the upstream solar wind in the 40 min after Cassini's crossing of SF and closest approach. *Bertucci et al.* [2015] proposed that the fossilization of magnetic field lines in Titan's ionosphere from the pre-SF solar wind plasma with higher dynamic pressure may be responsible for the large magnetic pileup.

Since Cassini's remaining Titan flybys (T114–T126) will all take place in Saturn's downstream region, T96 will remain the only case of Titan being observed in the supersonic solar wind. In this study we model Titan's plasma interaction with the solar wind during T96 using a hybrid model and compare our results against Cassini magnetic field and electron data. We investigate the possible contribution of fossilized fields to the observed magnetic field perturbations and study the robustness of Titan's induced magnetosphere against the observed nonstationarities in the incident solar wind conditions.

The coordinate system used throughout this study is the Titan-centered solar wind interaction system (TSWIS) introduced in *Bertucci et al.* [2015]. In this system the *x* axis points antisunward, the *y* axis points in the direction of Saturn's orbital motion, and the *z* axis completes the right-handed system.

2. Model Description

We apply the hybrid code AIKEF [*Müller et al.*, 2011; *Feyerabend et al.*, 2015] in our simulations, which treats ions as particles and electrons as a massless, charge-neutralizing fluid. Due to the large ion gyroradii of the incident solar wind plasma (see Table 1), a kinetic model is necessary to accurately describe Titan's plasma interaction during the T96 encounter. The model used to describe Titan's ionosphere is the same as in our previous Titan simulations [*Feyerabend et al.*, 2015]. Key features of this approach include a wavelength-dependent photoionization model (EUV flux model for aeronomic calculations), a network of the most important chemical reactions [see *Feyerabend et al.*, 2015, Table 2] and elastic collisions of ions with Titan's neutral atmosphere. Titan's nightside ionosphere is generated by electron impact ionization. Titan's ionosphere is described by a seven-species ion model, representing the different mass regimes of the observed ion distribution in the ionosphere [see *Feyerabend et al.*, 2015, Table 1].

Five simulations with different upstream parameters are discussed in this study. A summary of the parameters for each run is provided in Table 1. All simulations have been performed using a cubic $-4R_T < x, y, z < 4R_T$ box with a maximum resolution of 80 km in Titan's ionosphere. The upstream solar wind bulk velocity $\underline{U}_0$ is parallel to the *x* axis in all runs. There are two main differences between the parameters of the five simulations. First, the orientation of the upstream magnetic field is chosen to correspond to the different magnetic field regimes observed during the encounter: inbound and outbound of closest approach as well as upstream of the shock front (SF) Cassini encountered about 40 min before the flyby. The averaging intervals for the different magnetic field vectors are noted in Table 1. Second, the dynamic pressure of the incident solar wind (and hence the Mach number) is treated as a free parameter to achieve the best possible agreement between simulation results and Cassini observations of magnetic field and electron density.

The solar wind in run #1 has the lowest dynamic pressure (0.24 nPa), comparable to the pressure estimated from Cassini observations downstream of SF between 00:01 and 00:23 [*Bertucci et al.*, 2015]. The parameters of run #2 are identical to those of run #1 apart from a higher dynamic pressure of 0.64 nPa, which was obtained by changing the density and velocity of the incoming solar wind protons. Runs #3–#5 apply an even more enhanced dynamic pressure (1.5 nPa). The upstream magnetic field vector in runs #1–#3 has been calculated from the interval after the crossing of SF (00:01) and Cassini's entry into the Titan interaction region (00:23). Run #4 applies a magnetic field vector obtained from the outbound segment of the Cassini encounter, but before the spacecraft crossed Saturn's bow shock and left the supersonic solar wind [cf. *Bertucci et al.*, 2015, Figure 2]. The outbound field has a north-south and east-west orientation and forms an angle of 32° with the inbound magnetic field, another piece of evidence for nonstationary behavior.

Run #5 represents the magnetic conditions of the pre-SF regime, where the interplanetary magnetic field pointed mostly in the west-east direction (time interval 23:35–23:55 on 30 November 2013). The pre-SF field was also about a factor of 2 weaker than the post-SF field. Cassini left the pre-SF regime about 40 min before closest approach, and therefore, Titan was not directly exposed to these upstream conditions at the time of

Table 1. Plasma Parameters of the Simulation Runs[a]

Quantity	Run #1	Run #2	Run #3	Run #4	Run #5
Solar wind density n_{0,H^+} (cm^{-3})	0.7	1.9	1.5	1.5	1.5
Solar wind velocity U_0 (km/s)	460	450	770	770	770
Dynamic pressure p_0 (nPa)	0.24	0.64	1.5	1.5	1.5
Magnetic field strength B_0 (nT)	0.85	0.85	0.85	1.13	0.42
Magnetic field vector $\underline{B}_0/B_0$	(0.3, 0.36, −0.88)	(0.3, 0.36, −0.88)	(0.3, 0.36, −0.88)	(0.66, 0.54, −0.51)	(0.15, −0.94, 0.1)
Averaging interval for $\underline{B}_0$	1 Dec 00:01 – 00:23	1 Dec 00:01 – 00:23	1 Dec 00:01 – 00:23	1 Dec 01:55 – 02:35	30 Nov 23:35 – 23:55
Upstream proton Gyroradius (R_T)	2.19	2.14	3.66	2.75	7.42
Alfvén Mach number M_A	21	33	51	38	123
Magnetosonic Mach number M_{MS}	13	19	31	27	37
Description	low-pressure inbound field	intermediate-pressure inbound field	high-pressure inbound field	high-pressure outbound field	high-pressure pre-SF field
Color	green	orange	red	violet	blue

[a]The solar wind is assumed to consist of protons and electrons in all cases. An electron and proton temperature of 1 eV is used for the solar wind plasma.

the encounter. However, fossilized magnetic fields from the pre-SF regime may still have been trapped in Titan's ionosphere when Cassini passed by the moon [*Neubauer et al.*, 2006]. Due to computational constraints on the simulation runtime, a hybrid code cannot resolve the real-time evolution of putative fossilized fields over 40 min [see also *Müller et al.*, 2010]. Besides, any realistic inclusion of the magnetic field transition at SF in a local plasma simulation needs to fulfill the $\nabla \cdot \underline{B} = 0$ condition across the discontinuity. This requires knowledge of the *three-dimensional* structure of the magnetic field on both sides of SF [*Simon et al.*, 2009], which could not be measured by a single spacecraft. However, run #5 will illustrate the stationary structure of Titan's induced magnetosphere in the pre-SF regime and can therefore facilitate the identification of fossilized field signatures in T96 data.

The high dynamic pressures and Mach numbers of the solar wind used for the simulations (see Table 1) are motivated by the extreme upstream conditions during T96: the fact that Titan was located upstream of Saturn's bow shock for several hours indicates that the solar wind pressure was enhanced above usual levels. Very high Mach numbers of the solar wind have been observed during several Cassini crossings of Saturn's bow shock, and the values used in this study are consistent with the observed values [*Masters et al.*, 2011; *Sulaiman et al.*, 2015].

3. Model Results and Discussion

A three-dimensional overview of the magnetic field components, the plasma bulk velocity, and the electron number density for run #3 is given in Figure 1, where we also indicate the Cassini trajectory. During T96, Cassini was moving mainly in north-south direction and toward Saturn, approaching Titan from the upstream side and from high northern latitudes, with a superimposed motion in the $+y$ direction. The closest approach occurred in Titan's dayside hemisphere. The plasma quantities from run #3 are also plotted in Figure 2 for two planes which are referred to as the *flyby plane* and the *gyroplane*. The flyby plane contains the center of Titan as well as the Cassini trajectory, while the gyroplane is defined by the center of Titan, the undisturbed upstream velocity vector $\underline{U}_0$, and the convective electric field vector $\underline{E}_0 = -\underline{U}_0 \times \underline{B}_0$. Since the upstream magnetic field $\underline{B}_0$ is mainly north-south oriented, $\underline{E}_0$ is almost aligned with the $-y$ axis.

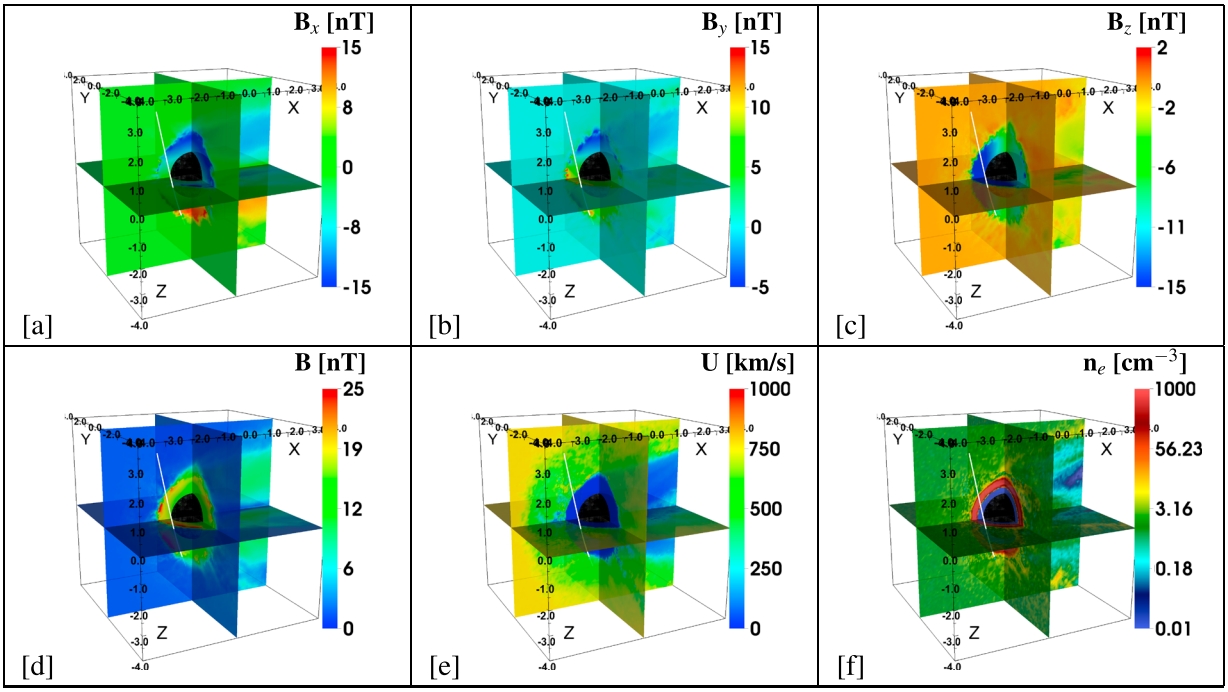

Figure 1. Plasma quantities of run #3 in the $x = 0$, $y = 0$, and $z = 0$ planes. (a–d) Magnetic field components and magnitude, (e) plasma bulk velocity, and (f) electron number density. The T96 trajectory is represented by the solid white line.

Figures 1 and 2 show the general structure of Titan's induced magnetosphere, which includes a bow shock (e.g., Figure 1d) and a magnetic barrier of enhanced field strength on the ramside. In the magnetic field observations, the bow shock was identified through short-scale oscillations in all three components (see also *Bertucci et al.* [2015] for a detailed description). Due to the limited grid resolution, the fine structure of the shock region is not reproduced by the model. The plasma velocity is greatly reduced in the vicinity of Titan due to the mass loading with freshly produced ionospheric and exospheric ions (Figures 2e and 2k). The location of Titan's bow shock overlaps with the extended mass loading region on the ramside. The filamented structure of the plasma quantities (e.g., Figures 2c, 2e, and 2f) on the upstream side of the bow shock is an indication of reflected solar wind particles [see also *Bößwetter et al.*, 2004]. Runs #1, #2, and #4 yield qualitatively similar results as run #3, with mostly quantitative differences. Therefore, no two-dimensional cuts are displayed for these runs.

Figure 3 compares the modeled magnetic field components $\underline{B} = (B_x, B_y, B_z)$ and the electron number density n_e from all five simulation runs against observations from the Cassini magnetometer [*Dougherty et al.*, 2004] and the electron number density, inferred from Langmuir Probe data and measurements of the upper hybrid frequency by the Radio and Plasma Wave Science Instrument (RPWS) [*Gurnett et al.*, 2004]. As can be seen, the magnitude and extension of the field perturbations in B_x, B_z, and $|\underline{B}|$ are reasonably well reproduced by runs #2–#4. The model also succeeds in reproducing the two maxima of the M-like perturbation signature seen in B_y. In addition, the location, magnitude, and width of the electron density enhancement observed near closest approach are in excellent quantitative agreement with the output of model runs #3–#5.

Since the upstream magnetic field pointed mainly in the north-south direction, the draping pattern shows a negative B_x component in the northern hemisphere ($z > 0$) and a positive B_x component in the southern hemisphere ($z < 0$), as can be seen in Figures 1a and 2a. However, due to the nonzero $B_{0,x}$ and $B_{0,y}$ components of the upstream field the draping pattern is slightly asymmetric with respect to $z = 0$ and also features a weak B_y perturbation. Cassini only grazed the outer regions of Titan's northern magnetic lobe in the inbound segment ($B_x < 0$, between 00:32 and 00:36), followed by an extended passage through Titan's southern magnetic lobe ($B_x > 0$, between 00:36 and 00:57). This bipolar feature in B_x is found in all simulation runs that use an upstream magnetic field from a time interval close to the encounter (runs #1–#4, Figure 3).

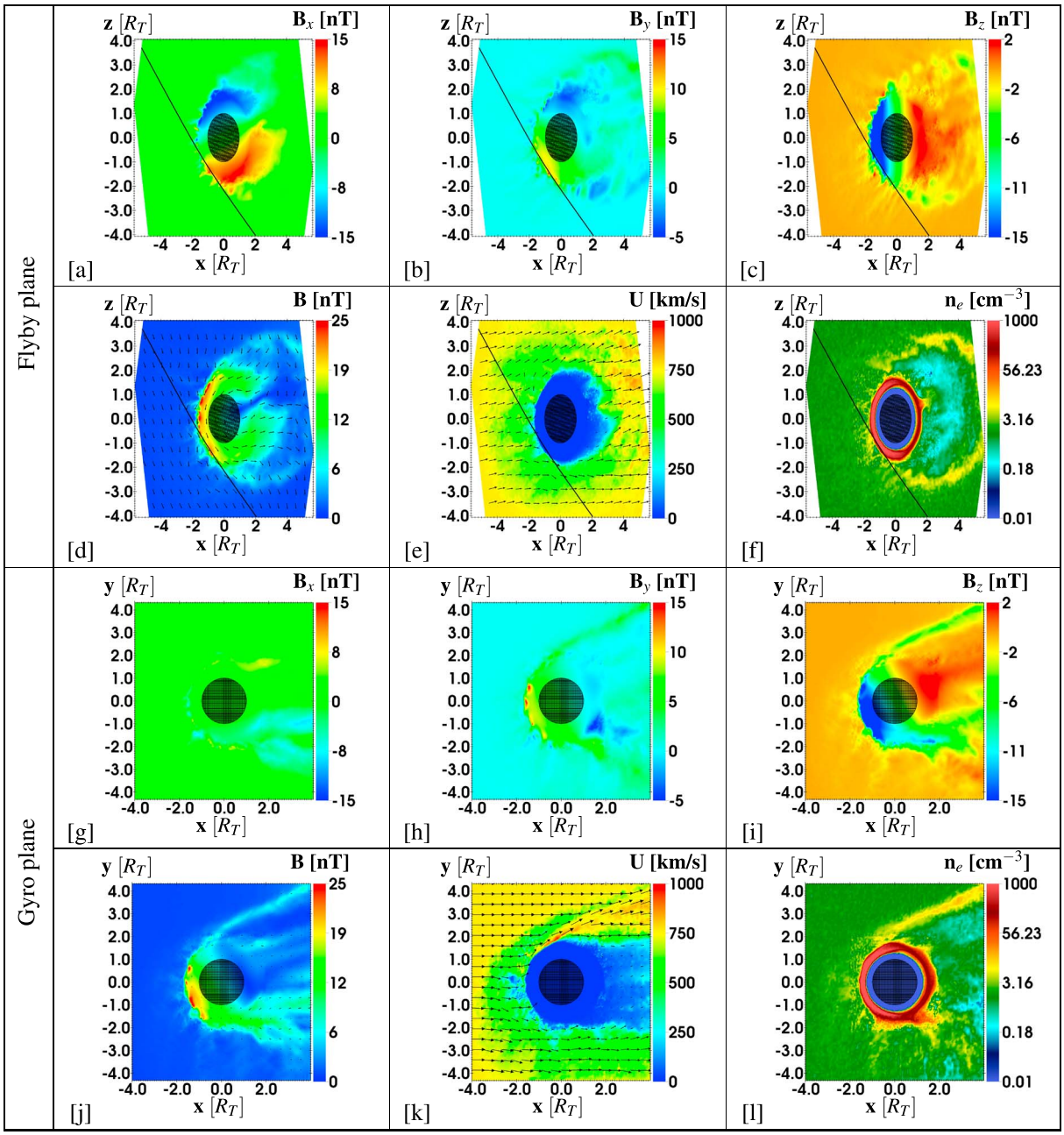

Figure 2. Plasma quantities of run #3 in the flyby and gyroplane. (a–d and g–j) Magnetic field components and magnitude, (e and k) plasma bulk velocity, and (f and l) electron number density. Arrows denote the projection of the respective vector field on the cutting plane. The nonrectangular shape of the flyby plane arises from its inclination against the coordinate axes in the cubic simulation domain.

The spacecraft did not penetrate below the magnetic ionopause, since no dropout of the magnetic field strength was observed near closest approach. This is consistent with our simulations (see Figures 2d and 3). Since the flyby took place in Titan's upstream region, Cassini did not intersect the wakeside plasma tail of Titan nor regions of enhanced ion outflow in the plane perpendicular to the upstream magnetic field (see Figures 1, 2k, and 2l).

As can be seen in Figure 3, the low-pressure run #1 produces draping and pileup signatures that are *qualitatively* consistent with the observations. However, the magnitude of the modeled field enhancement is not large enough to explain the data ($|\underline{B}|$<15 nT in the model compared to the observed maximum value of $|\underline{B}|$ ~25 nT at 00:41). In addition, the modeled electron density enhancement in run #1 is too broad to

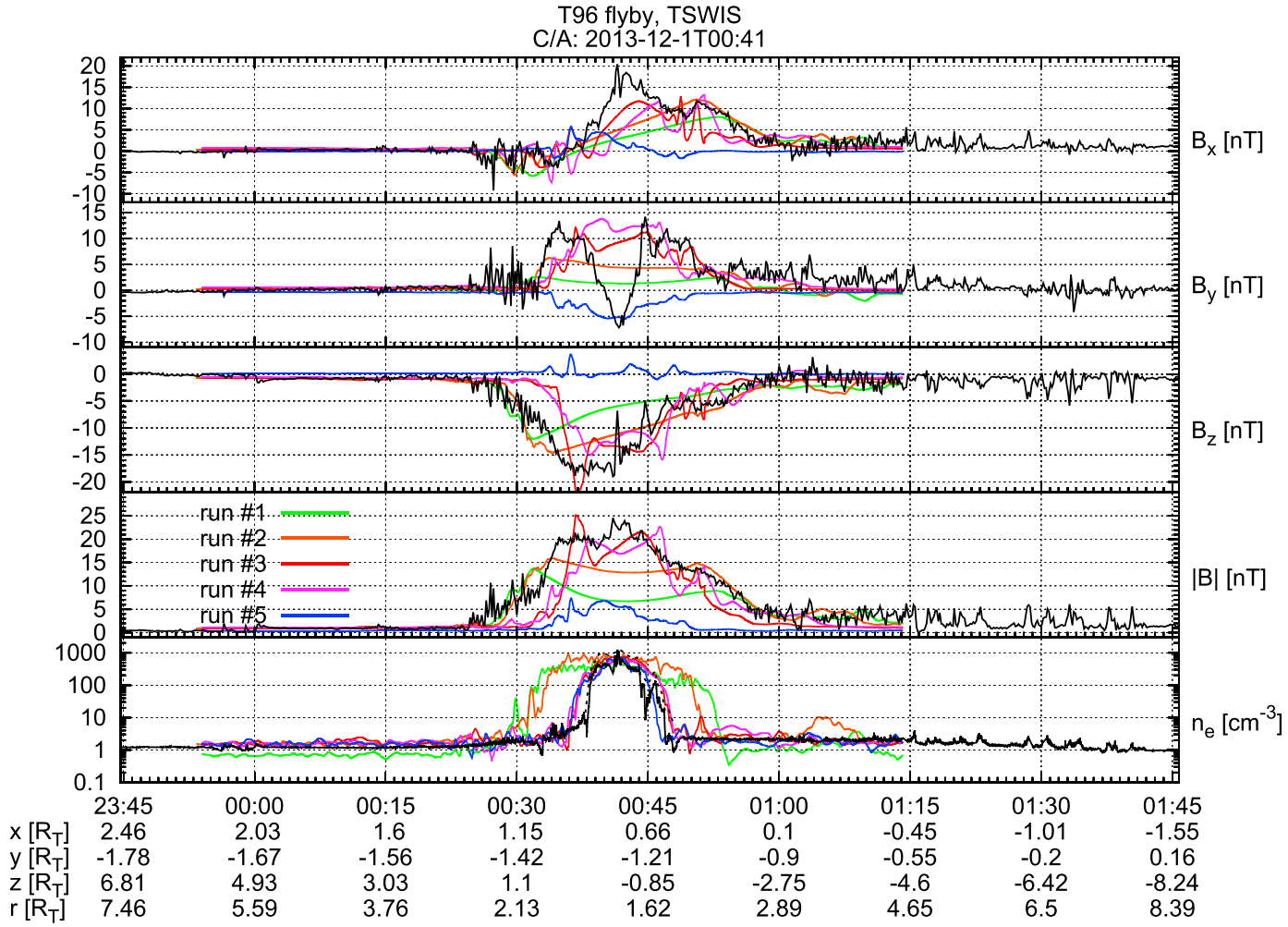

Figure 3. Modeled magnetic field components (B_x, B_y, B_z) and electron number density n_e for all five runs compared against the T96 Cassini observations. Observations are displayed in black. For the electron density data, the solid black line refers to LP data, while the dashed black line refers to densities obtained from the upper hybrid frequency. TSWIS coordinates and distance r to Titan's center of Cassini during the flyby are displayed for their respective time points.

be consistent with the observed density pattern. Only the peak density is of the same magnitude as observed. Thus, the low-pressure upstream conditions of run #1 are not able to quantitatively explain the data and indicate that a higher dynamic upstream pressure is needed.

Run #2 therefore applies a higher upstream pressure of 0.64 nPa, which was proposed by *Bertucci et al.* [2015] based on pressure balance calculations for Titan's magnetic barrier. Figure 3 shows that this increased upstream pressure yields a much better agreement with the magnetic field observations. Yet while the magnitude of the observed electron density enhancement is again well reproduced, the modeled electron density signature is still too broad. It should be noted as well that the chosen upstream magnetic field (from the segment after the SF), in general, leads to a positive B_y perturbation along the Cassini trajectory that cannot explain the dip in the middle of the observed M-shaped B_y signature. The reasons for this discrepancy will be discussed later.

Another increase in the solar wind dynamic pressure to 1.5 nPa in run #3 (also used in runs #4 and #5) is able to push the region of enhanced ionospheric electron density farther toward the moon, thereby yielding excellent agreement with the observed box-like density enhancement. We note again that runs #1–#3 use the upstream magnetic field obtained from the inbound part of the encounter, i.e., between the crossing of SF and closest approach.

To investigate the effects of the observed rotation of the ambient solar wind magnetic field during the encounter, in run #4 an upstream magnetic field obtained from the outbound segment was applied

(cf. Table 1). As can be seen in Figure 3, this leads to only minor quantitative changes in the modeled magnetic field components. The modeled electron density is almost identical to run #3 as well. Using the outbound magnetic field yields slightly better agreement between modeled and measured $|\underline{B}|$ in the outbound segment of the flyby, whereas the inbound field in run #3 gives better agreement with the inbound draping pattern in B_x than run #4. Overall, the magnetic and density features in both runs look very similar. Both, runs #3 and #4, produce a plateau-like enhancement in B_y. The width of this plateau agrees well with the width of the observed perturbation region in B_y. The magnitude of the modeled B_y enhancement is consistent with that of the two spikes seen in B_y by the magnetometer.

Hence, runs with a high solar wind pressure and an upstream magnetic field obtained from a time interval *after* the SF are able to quantitatively reproduce numerous key features of the observed magnetic field signatures as well as the magnitude and width of the electron density enhancement around closest approach to Titan. Overall, the simulated interaction signatures along the T96 trajectory exhibit a high level of robustness against the observed changes of the incident flow conditions. Since we use the solar wind dynamic pressure as a free parameter to achieve the best possible agreement between model and data, similar results could also be obtained by using a different combination of solar wind density and flow speed. The only feature of the observed magnetic field signature that could not yet be explained is the dip in the middle of the M structure seen in B_y around closest approach between 00:38 and 00:44. In this region, the B_y component drops from positive values of about ~10 nT at the two "spikes" of the M to negative values with a minimum of −7 nT at closest approach.

The draping of the north-south oriented solar wind magnetic fields from runs #1–#4 generates a plateau-like positive B_y perturbation near closest approach. However, this plateau is only consistent with the observations at the two outer spikes of the M signature between 00:33 and 00:38 as well as 00:44 and 00:50 where the observed B_y is also positive.

Since the previously used upstream magnetic field vectors give good agreement in all components except for the inner dip of the M signature in B_y, it is unlikely that this feature could be caused by, e.g., short-scale fluctuations or a different geometry of the upstream magnetic field and plasma bulk velocity. Given that B_y drops by about 17 nT in the center of the M signature, one would then expect to see related perturbations in the other magnetic field components as well.

The extent of the dip in B_y is symmetric around closest approach at 00:41 and covers altitudes of 1800 km to 1400 km. Due to the combination of low plasma velocity and sufficiently large magnetic Reynolds number, this altitude regime of Titan's ionosphere may store fossilized magnetic field lines most efficiently [*Neubauer et al.*, 2006]. *Bertucci et al.* [2008] suggest the lifetimes of such fossilized field signatures to range between 20 min and up to 3 h. Hence, we propose that remnants of a previously encountered upstream magnetic field configuration are responsible for the inner dip of the M feature in B_y.

To substantiate this hypothesis, the upstream magnetic field in run #5 was obtained from the interval immediately prior to Cassini's crossing of the SF (23:35–23:55 on 30 November 2013 [cf. *Bertucci et al.*, 2015, Figure 2]. In this regime the magnetic field vector possessed a strong west-east ($-y$) component. Compared to runs #1–#4, Titan's magnetic lobes in such an upstream field are rotated around the x axis by 90° and can now be found in the $y<0$ and $y>0$ half-spaces. The ramside magnetic barrier is mainly visible in the B_y component. As can be seen in Figure 3, this upstream field therefore results in a broad negative B_y perturbation along Cassini's trajectory with a minimum value of $B_y \approx -5$ nT around closest approach. The strength and orientation of this negative B_y perturbation are in agreement with Cassini observations at the "bottom" of the M-like signature. The perturbations in the B_x and B_z components are much smaller than in runs #1–#4. Especially, around closest approach the B_x and B_z components from run #5 are almost completely undisturbed.

Above altitudes of 1800 km, Titan's induced magnetosphere can adapt to a change of the ambient magnetic field orientation from west-east (pre-SF) to north-south (post-SF) on timescales of only a few minutes [*Simon et al.*, 2009]. Thus, the outer layers of the magnetic pileup region are quickly eroded through convection and reconnection by such a rotation of the upstream field. However, the pre-SF pileup at Titan's ramside (mainly visible in B_y and *not* in B_z) may prevail at altitudes below 1800 km for several hours. We therefore propose that draped field lines from the pre-SF regime were still present in Titan's lower ionosphere at closest approach (i.e., 40 min after Cassini's crossing of SF) and gave rise to the inner dip of the M-like signature in B_y.

Although the reconfiguration of Titan's induced magnetosphere during a rotation of the upstream magnetic field is a highly nonlinear process, the low convection speeds in the moon's deep ionosphere shield the magnetic draping pattern in that region to a certain degree against changes in the incident flow conditions [*Neubauer et al.*, 2006; *Bertucci et al.*, 2008; *Simon et al.*, 2009]. We note that the "summit" of the observed B_x draping pattern (which we could not quantitatively reproduce, see Figure 3) is located at the same position as the proposed fossilized magnetic field signature in B_y. It is very well possible that this overshoot in B_x arises from the deformation of the fossilized field lines between the time of their "capture" and the time of their subsequent detection by Cassini.

4. Concluding Remarks

Our simulations show that the outer part of Titan's induced magnetosphere at the time of T96 is consistent with the picture of a quasi-stationary interaction between the moon's ionosphere and a high-pressure solar wind flow, as used in runs #3 and #4. However, we also provide strong evidence that the fine structure of the magnetic field in Titan's deep ionosphere was governed by fossilized magnetic field lines. These field lines could have been trapped in Titan's ionosphere at least 40 min before the T96 encounter took place. A lifetime of 40 min agrees well with the time window inferred by *Bertucci et al.* [2009] from the first in situ detection of fossilized magnetic fields during the T32 magnetosheath excursion.

Acknowledgments
The work of Moritz Feyerabend, Sven Simon, and Uwe Motschmann was financially supported by the Deutsche Forschungsgemeinschaft (DFG) under grant SI1753/1-1. The research at the University of Iowa was supported by NASA through contract 1415150 with the Jet Propulsion Laboratory. The Cassini MAG and RPWS data sets displayed in Figure 3 can be obtained from the *Planetary Data System*. The simulation data and the source code used to generate Figures 1–3 are available from first author Moritz Feyerabend upon request.

References

Bertucci, C., et al. (2008), The magnetic memory of Titan's ionized atmosphere, *Science*, *321*(5895), 1475–1478, doi:10.1126/science.1159780.

Bertucci, C., B. Sinclair, N. Achilleos, P. Hunt, M. K. Dougherty, and C. S. Arridge (2009), The variability of Titan's magnetic environment, *Planet. Space Sci.*, *57*(14–15), 1813–1820, doi:10.1016/j.pss.2009.02.009.

Bertucci, C., F. Duru, N. Edberg, M. Fraenz, C. Martinecz, K. Szego, and O. Vaisberg (2011), The induced magnetospheres of Mars, Venus, and Titan, *Space Sci. Rev.*, *162*, 113–171, doi:10.1007/s11214-011-9845-1.

Bertucci, C., D. C. Hamilton, W. S. Kurth, G. Hospodarsky, D. Mitchell, N. Sergis, N. J. T. Edberg, and M. K. Dougherty (2015), Titan's interaction with the supersonic solar wind, *Geophys. Res. Lett.*, *42*, 193–200, doi:10.1002/2014GL062106.

Bößwetter, A., T. Bagdonat, U. Motschmann, and K. Sauer (2004), Plasma boundaries at Mars: A 3-D simulation study, *Ann. Geophys.*, *22*, 4363–4379.

Dougherty, M. K., et al. (2004), The Cassini magnetic field investigation, *Space Sci. Rev.*, *114*, 331–383, doi:10.1007/s11214-004-1432-2.

Edberg, N. J. T., et al. (2013), Extreme densities in Titan's ionosphere during the T85 magnetosheath encounter, *Geophys. Res. Lett.*, *40*, 2879–2883, doi:10.1002/grl.50579.

Feyerabend, M., S. Simon, U. Motschmann, and L. Liuzzo (2015), Filamented ion tail structures at Titan: A hybrid simulation study, *Planet. Space Sci.*, *117*, 362–376, doi:10.1016/j.pss.2015.07.008.

Gurnett, D. A., et al. (2004), The Cassini radio and plasma wave investigation, *Space Sci. Rev.*, *114*, 395–463, doi:10.1007/s11214-004-1434-0.

Masters, A., S. J. Schwartz, E. M. Henley, M. F. Thomsen, B. Zieger, A. J. Coates, N. Achilleos, J. Mitchell, K. C. Hansen, and M. K. Dougherty (2011), Electron heating at Saturn's bow shock, *J. Geophys. Res.*, *116*, A10107, doi:10.1029/2011JA016941.

Müller, J., S. Simon, U. Motschmann, K. H. Glassmeier, J. Saur, J. Schuele, and G. J. Pringle (2010), Magnetic field fossilization and tail reconfiguration in Titan's plasma environment during a magnetopause passage: 3D adaptive hybrid code simulations, *Planet. Space Sci.*, *58*(12), 1526–1546, doi:10.1016/j.pss.2010.07.018.

Müller, J., S. Simon, U. Motschmann, J. Schüle, K. Glassmeier, and G. J. Pringle (2011), A.I.K.E.F.: Adaptive hybrid model for space plasma simulations, *Comput. Phys. Commun.*, *182*(4), 946–966, doi:10.1016/j.cpc.2010.12.033.

Neubauer, F. M., et al. (2006), Titan's near magnetotail from magnetic field and plasma observations and modelling: Cassini flybys TA, TB and T3, *J. Geophys. Res.*, *111*, A10220, doi:10.1029/2006JA011676.

Simon, S., U. Motschmann, G. Kleindienst, J. Saur, C. Bertucci, M. Dougherty, C. Arridge, and A. Coates (2009), Titan's plasma environment during a magnetosheath excursion: Real-time scenarios for Cassini's T32 flyby from a hybrid simulation, *Ann. Geophys.*, *27*(2), 669–685.

Sulaiman, A. H., A. Masters, M. K. Dougherty, D. Burgess, M. Fujimoto, and G. B. Hospodarsky (2015), Quasiperpendicular high mach number shocks, *Phys. Rev. Lett.*, *115*, 125001, doi:10.1103/PhysRevLett.115.125001.